Fractal characterization of two-dimensional aluminum corrosion fronts

Terje Holten, Torstein Jøssang, Paul Meakin, and Jens Feder
Department of Physics, University of Oslo, P.O. Box 1048 Blindern, N-0316 Oslo, Norway
(Received 6 January 1994)

The corrosion of aluminum foils in a two-dimensional cell has been investigated experimentally. The corrosion was allowed to attack from only one side of an otherwise encapsulated metal foil. A 1*M* NaCl (pH = 12) electrolyte was used and the experiments were controlled potentiostatically. Experiments were performed at two different potentials. Photographs from the experiments were digitized and the interfaces between the electrolyte and metal (the corrosion fronts) were identified. The corrosion fronts were analyzed using four different methods, which showed that the fronts can be described in terms of self-affine fractal geometry over a significant range of length scales. The width as a function of length showed self-affine scaling with a Hurst exponent of 0.65 ± 0.05 for both fronts. Results from corrosion experiments using zinc and copper are briefly mentioned.

PACS number(s): 05.70.Ln, 81.60.Bn, 68.55.Jk

In recent years, fractal geometry has been used to describe a wide variety of natural phenomena [1,2]. Fractal geometry can also describe certain types of electrodeposition morphologies. The growth of disorderly patterns during electrodeposition has been studied extensively in recent years and a variety of morphological regimes and transitions have been found [3,4]. There has been no similar systematic experimental study of corrosion patterns, in spite of the obvious relationship to electrodeposition. Various types of corrosion models have been studied using theoretical methods and computer simulations. These include dealloying [5,6], pitting [7,8], and electropolishing [9] models.

The study of corrosion is a large enterprise that has focused on electrochemical processes and on electrical currents and potentials. There has been substantial interest in the morphology of corrosion interfaces but little quantitative work has been done on either the structure or dynamics of corrosion fronts. The corrosion front itself defines the boundary conditions of the growth, which is an important parameter for the transport of ions and corrosion products. For practical reasons, most of the research has been carried out using three-dimensional systems. A study of a steel pipe subjected to CO_2 corrosion revealed indications of a self-affine geometry [10]. A three-dimensional reconstruction was made by digitizing photographs of a sequential grinding of the surface. Hurst exponents in the range of 0.8–0.9 were measured from height difference correlation functions. The Hurst exponents varied with the position of the cut, indicating an inhomogeneous surface. Costa, Sagués, and Vilarrasa [11] have studied the shapes of pit boundaries of stainless steel in synthetic ocean water. The steel was corroded at a temperature of 25 °C and a potential of 250 mV with respect to the standard Calomel electrode (SCE). A crossover from a fractal dimensionality of about 1.17 on short length scales to about 1.41 on longer scales was observed. However, the total range of length scales was quite small. One-dimensional experimental systems (metal electrodes in a glass capillary) have been used to model pitting corrosion. Two-dimensional models do not appear to have been used before. Corrosion structures can be difficult to study because corrosion is often a very slow process and corrosion products often hinder observations.

Aluminum is protected by an oxide layer in most environments [12] and is therefore suitable for studies of pitting corrosion. In addition, the pitting corrosion of aluminum and aluminum alloys in chloride containing aqueous electrolytes is an important practical problem. Pitting corrosion can lead to rough surfaces because of the formation and decay of a protective layer. Kaesche [13] found that the potential above which Al undergoes pitting corrosion in 1*M* NaCl is -0.48 V with respect to the standard hydrogen electrode (SHE) [-0.72 V (SCE)]. The potentials in our experiments are well above this potential. Frankel [14] has studied the growth of pits in thin aluminum films. A 100–200 nm thick Al film on a quartz substrate was exposed to a chloride solution from above. Pits grew in the thin film samples and quickly penetrated the film. At low potentials, the pit perimeters were convoluted and at higher potentials [above about -0.58 V (SCE)], the pit perimeters became round and smooth. The surface was not analyzed in more quantitative terms. Elola, Otero, and Porro [15] have studied the pitting of commercially pure aluminum exposed to the atmosphere. They found that the average pit depth grew algebraically with increasing time with exponents between 0.14 and 0.19. When aluminum is corroded in chloride containing aqueous solutions, the Al^{3+} ion undergoes hydrolysis [16], the pH near the electrode decreases to a value of 3–4, and the compounds $Al(OH)_2Cl$ and $Al(OH)Cl_2$ are formed.

We have carried out experiments using a two-dimensional cell in which corrosion can take place along only one exposed edge of a metal foil. All other sides except this edge are protected by an epoxy coating. Figure 1 shows a schematic representation of the corrosion cell.

High purity aluminum foils (from Goodfellow) of size 5×2.5 cm^2 and thickness 50 μm were used. The edge

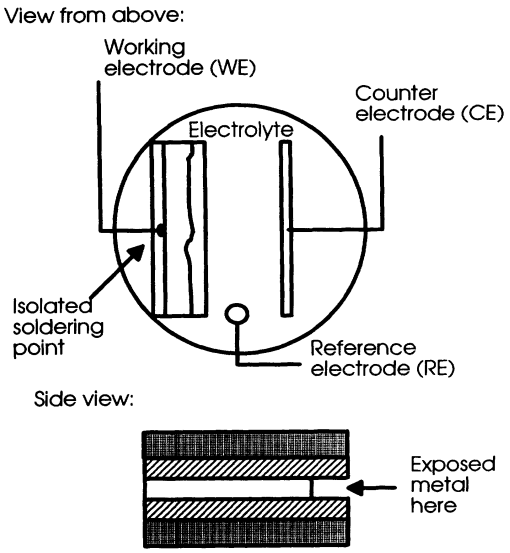

FIG. 1. A schematic representation of the experimental setup. Above: The cell is viewed from above. Below: The corrosion cell, viewed from one side. Additional glass slides were added on top of and beneath the cell to prevent electrolyte and corrosion products from obscuring the view.

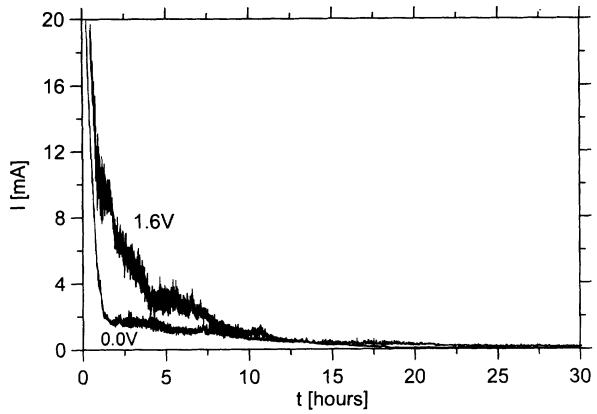

FIG. 2. The current I as function of time t for aluminum foils corroded in 1M NaCl (pH=12) with potentials of 0.0 V (SCE) and 1.6 V (SCE), respectively.

that was initially exposed to corrosion was 5 cm long. The foils were annealed at 450 °C for 1 h. Both sides of the metal were glued with corrosion resistant epoxy to a glass slide that protects the metal from corrosion, from above and below. The metal and epoxy sticking out from one edge of the glass slides were removed by rubbing with wet sand paper (P320), leaving a straight metal edge. A copper wire was connected to the metal, and the soldering point was totally covered with epoxy. The enclosed foil was placed in the middle of a stack with a total of 13 glass slides that reached the lid of the cell. In this way photographs could be taken while the experiment was running because corrosion products could not deposit on top of the enclosed electrode. This electrode (the working electrode, WE) was placed in a 9 cm diameter petri dish. The counter electrode (CE), made of the same metal as the WE, was placed vertically and stuck through a slit in the lid. The reference electrode (RE) was placed slightly off to one side near the WE and the petri dish was filled with electrolyte.

A 1M NaCl+0.01M NaOH (pH=12) electrolyte was used. The experiments were carried out under potentiostatic control (the potential difference between the WE and RE was kept constant). The potentials with respect to the SCE reference electrode were 1.6 or 0.0 V. Current records from these experiments are shown in Fig. 2. The current fluctuations in the 1.6 V experiment can be seen in this figure. The front seemed to be more homogeneous in the 0.0 V experiment. There were small fragments of aluminum that had become disconnected from the main body of the aluminum foil near the corrosion fronts in both experiments. The average corrosion depth in the 0.0 V experiment was about half the depth in the 1.6 V experiment.

The experiments were stopped after 30 h. Six partly overlapping pictures from each experiment were digitized, and the corrosion fronts were identified. The six corrosion fronts were then fitted together with a computer program to reconstruct an image of a 1.4 cm section of the corrosion front. A horizontal resolution of 1 μm was obtained corresponding to about 14 000 pixels in the horizontal direction. The photographic negatives were digitized using a film scanner (Nikon LS 3500) connected to an Apollo work station. All photographs were digitized with a resolution of 3000×2000 pixels. The corrosion fronts were identified using our own image processing software. Photographs of the corrosion fronts are shown in Fig. 3.

These corrosion fronts were analyzed using four different methods. Table I shows the Hurst exponents

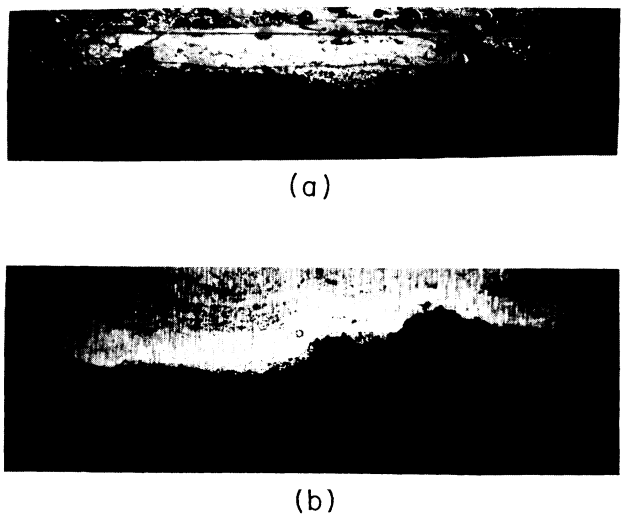

FIG. 3. Two photographs of aluminum corrosion fronts in a 1M NaCl (pH=12) solution (the metal is black). The potentials were (a) 0.0 V (SCE), and (b) 1.6 V (SCE). These pictures show the parts of the corrosion fronts that were analyzed. Six partly overlapping pictures from each front shown were fitted together to obtain a high resolution image. The horizontal scale is about 14 mm and consists of about 14 000 pixels.

TABLE I. The Hurst exponent H measured from the different analysis methods at the two different potentials. The Hurst exponent from the box-counting analysis was calculated from the box-counting dimension D with the formula $H=2-D$. The errors are estimated to ± 0.05.

Measure	0.0 V	1.6 V
$w(L)$	0.65	0.65
$C_2(L)$	0.55	0.68
$S(k)$	0.68	0.66
$N(\delta)$	0.78	0.83

measured by these methods at the two potentials. The Hurst exponents were measured for (horizontal) length scales in the range $L_{\min} \leq L \leq L_{\max}$. A lower limit ($L_{\min}$) of 50 μm was chosen to avoid film thickness effects (except for the power spectra analyses), even though some of the log-log plots appear to be linear down to much smaller length scales. $L_{\max}$ is the upper limit to the range of horizontal length scales over which a reasonably good fit can be obtained. The ranges in which the data were fitted are marked with solid lines in all the relevant figures, and with dotted lines outside the fitting range. The estimated statistical errors of the Hurst exponents are similar for the different analysis methods and are typically about ± 0.05. In all methods used, except box counting, it is assumed that the overhangs can be neglected so that the front can be represented by a single-valued height profile $h(x)$. The minimum values of the height (corresponding to the deepest corrosion depth) were selected when an overhang was encountered. In most cases, the value obtained from H is not sensitive to whether the minimum, maximum, or mean values of the front heights are chosen.

The width $w(L)$ is defined as

$$w(L)=[\langle h^2(x)\rangle_L-\langle h(x)\rangle_L^2]^{1/2}, \tag{1}$$

where $\langle\ \rangle_L$ denotes an average over the length L. The width w scales as [17]

$$w(L)\sim L^H \tag{2}$$

for self-affine fractals. The width was measured as a function of the horizontal length L for the two corrosion fronts (Fig. 4). The result from the 1.6 V experiment can be fitted by Eq. (2) over a range of two and a half decades, giving $H=0.65$. The systematic deviations from the straight line reach a peak at about $L=50$ μm, which is equal to the foil thickness. At this thickness the system crosses over from three dimensional to two dimensional. The corrosion front width in the 0.0 V experiment follows a power law for $\log_{10}(L)<2.5$. The fit by Eq. (2) gives $H=0.65$.

The fronts were also analyzed by the second moment height difference correlation functions defined by [10]

$$C_2(L)=[\langle |h(x+L)-h(x)|^2\rangle]^{1/2}. \tag{3}$$

For self-affine fractals the correlation function $C_2(L)$ has the form

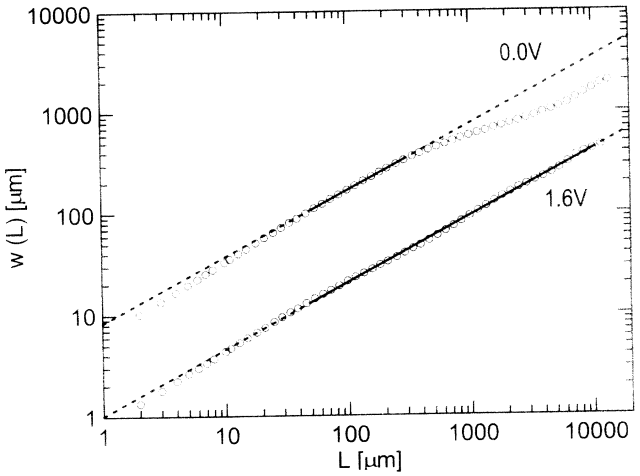

FIG. 4. The width w as a function of the length L for the corrosion fronts at the two different potentials (circles). The power law fits are straight lines in these log-log plots. The result from the 0.0 V experiment is shifted upwards by one decade for clarity.

$$C_2(L)\sim L^H. \tag{4}$$

Figure 5 shows the correlation functions $C_2(L)$ for the fronts. By fitting the measured correlation functions by Eq. (4), the effective Hurst exponents $H=0.68$ (1.6 V experiment) and $H=0.55$ (0.0 V experiment) were obtained. The effective Hurst exponent, determined from $C_2(L)$, depends on the range of length scales used in the least squares fit. The correlation lengths, $\xi_\parallel$ and $\xi_\perp$, in directions parallel and perpendicular to the direction along the surface can be defined as the location of the first crossover to a lower slope in Fig. 5. $\xi_\parallel$ and $\xi_\perp$ are about 0.1 and 0.06 mm, respectively, for the 0.0 V experi-

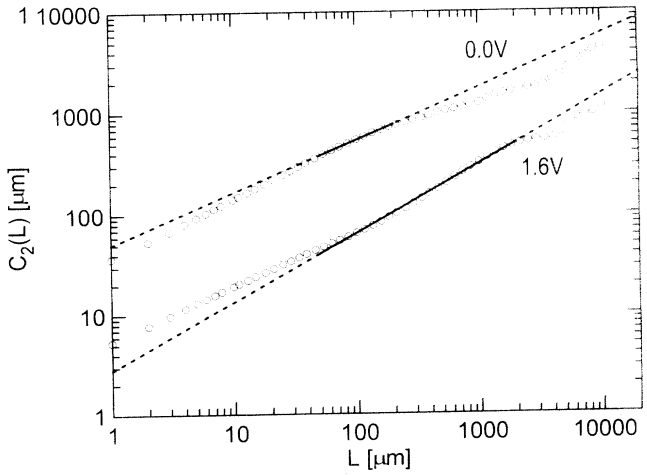

FIG. 5. The height difference correlation function $C_2(L)$ as a function of the length L for the two corrosion fronts (circles). The power law fits are straight lines in these log-log plots. The result from the 0.0 V experiment is shifted upwards by one decade for clarity.

ment and about 2 and 0.4 mm for the 1.6 V experiment. The correlation lengths, obtained when the experiments were repeated under the same conditions, are within a factor of 2 from these values.

The power spectrum $S(k)=|F(k)|^2$ of the Fourier components $F(k)$ of a self-affine single-valued height profile $h(x)$ has the form [2]

$$S(k)\sim k^{-1-2H} . \quad (5)$$

The fronts were divided into 13 (1.6 V experiment) or 14 (0.0 V experiment) parts each of 1024 pixels. The power spectra (Fig. 6) from these parts were averaged to decrease the noise [18]. The fits by Eq. (5) gave $H=0.66$ and 0.68 for the 1.6 and 0.0 V experiments, respectively. The power spectra were fitted in the range 10 $\mu m \leq L \leq 100$ μm. The averaging decreased the total range. Reasonable H values could not be obtained with L_{min} equal to 50 μm.

In the box-counting method [2], a set is covered by a grid of square boxes with sides of length δ. The number of boxes, $N(\delta)$, that contains at least one point in the set is counted. If the set is a self-similar fractal $N(\delta)$ scales as

$$N(\delta)\sim\delta^{-D} , \quad (6)$$

where D is the fractal dimension. Box-counting analysis of a self-affine fractal results in two different D values, $D=2-H$ at lengths smaller than a crossover length ξ, and $D=1$ on larger length scales [19]. The results from the box-counting analysis of the fronts are shown in Fig. 7. The results were fitted using Eq. (6), giving $D=1.17$ and 1.22 for the 1.6 and 0.0 V experiments, respectively. There are almost no deviations of the data from the fitting line for the first three decades. The crossover occurs when the box size reaches the maximum height difference $[\langle |h(x_0)-h(x_0+x_1)| \rangle \approx x_1 \approx \delta \approx \xi]$. The box-counting dimension D, obtained from a least squares fit over the first two decades, varies from 1.14 to 1.28 on the six individual parts of the 1.6 V experiment. An advantage of the box-counting method is that overhangs are not neglected.

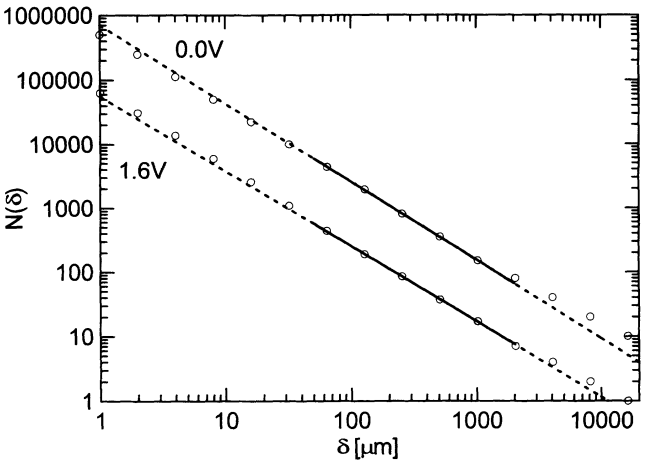

FIG. 7. The result of a box-counting analysis. The experimental data (circles) were fitted using Eq. (6). The result from the 0.0 V experiment is shifted upwards by one decade for clarity.

Twelve pictures were taken at different times from the 0.0 V experiment. A horizontal scale of 8 mm consisting of 3000 pixels was used corresponding to a resolution of about 2.7 μm. The Hurst exponent H was measured from the functions $w(L)$ and $C_2(L)$. The exponents were obtained by least squares fitting straight lines to the corresponding log-log plots in the interval 50 $\mu m \leq L \leq 200$ μm, over which all the functions have a power law form. Figure 8 shows the Hurst exponents as a function of time. This figure shows large fluctuations in the measured Hurst exponents. The H values measured from the front widths $w(L)$ are usually higher than the H values from the correlation function $C_2(L)$. The growth seems to be characterized by two different regimes; almost semicircular pits develop in the early stages of corrosion, and later the morphology is characterized by self-affine geometry. This behavior is most pronounced in the 1.6 V experiment. Additional experimental work is required to quan-

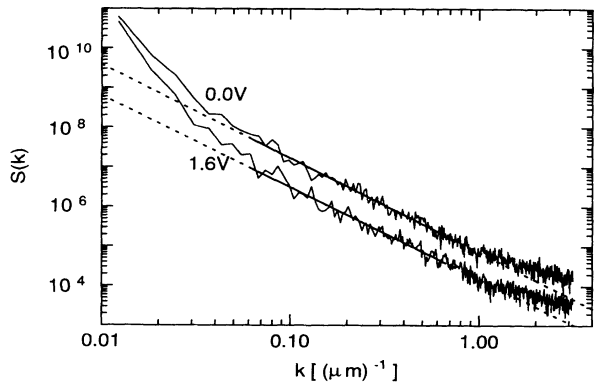

FIG. 6. The power spectrum $S(k)$ as a function of $k=2\pi/L$. The power spectra were averaged from 13 or 14 parts each of 1024 pixels from the fronts. The power law fits are represented by the straight lines in these log-log plots. The result from the 0.0 V experiment is shifted upwards by one decade for clarity.

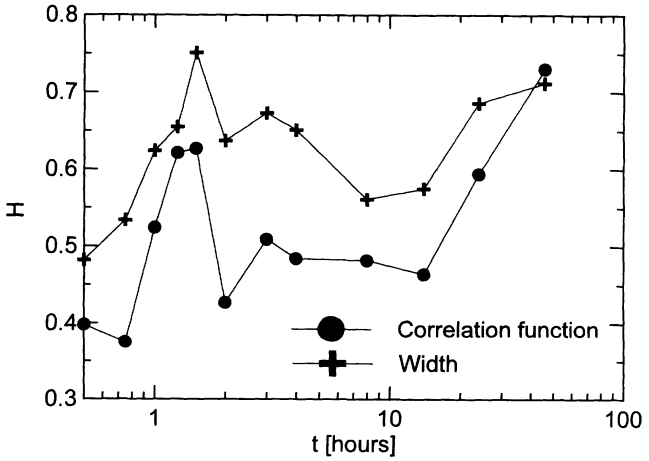

FIG. 8. The Hurst exponent H as a function of time t for the 0.0 V experiment. H was measured by fitting the functions $w(L)$ and $C_2(L)$ in the range 50 $\mu m \leq L \leq 200$ μm.

titatively characterize the growth and to find out if a simple growth model can be used to fit data averaged from several similar experiments.

All these results support the idea that the corrosion fronts can be quantitatively characterized by using self-affine fractal geometry. Except for the box-counting analysis, all the methods used to analyze the corrosion fronts from the 1.6 V experiment were consistent. The H values are more scattered for the 0.0 V experiment in which the correlation lengths $\xi_{\parallel}$ and $\xi_{\perp}$ are smaller. For any particular analysis method the Hurst exponents [except when measured from $C_2(L)$] are almost equal for the two potentials. The Hurst exponents measured by the box-counting method with the formula $H=2-D$ are higher than the exponents measured by the other methods. Visual inspection indicates that there are clear differences between the fronts but these differences do not appear to have much influence on the Hurst exponents. However, these differences are accounted for in terms of different correlation lengths in Fig. 5. It is possible that the corrosion fronts are fractal on length scales that are smaller than those studied here. However, the foil thickness limits the two-dimensional regime in which the geometric scaling properties can be measured using projections of the front onto the plane of the foil.

Corrosion experiments were carried out using zinc under similar experimental conditions. The potential was 2.0 V with respect to the SCE and the duration of the experiment was 24 h. A Hurst exponent of 0.68 ± 0.05 was measured from the correlation function $C_2(L)$.

Corrosion experiments were also performed using 25 μm thick copper foils in an alkaline solution [$0.05M$ $NaSO_4+0.088M$ NaOH (pH$=12.9$)] at a potential of 10.0 V with respect to a standard sulphate electrode (SSE). The current record was very "noisy" due to the formation of oxygen bubbles. A horizontal cut through the current record was a Cantor set [2] with a fractal dimension of 0.51 ± 0.05, fitted in the range of time scales between 1 and 50 s.

The quantitative characterization of corrosion front morphologies is an important step towards the development of a better understanding of the underlying physical and chemical corrosion mechanisms. Results from computer simulations that incorporate our understanding of the corrosion process can be compared to experimental data. Discrepancies between the simulations and the observed self-affine fractal corrosion front geometry could then be used to motivate refinements in the corrosion model. A better structural model for corrosion morphologies may also be of value in the development of improved statistical approaches to the prediction of lifetimes of different devices (such as underground pipelines) from measurements of corrosion products. In practice there is a rich phenomenology associated with corrosion processes. The front morphology can be expected to depend on the materials and conditions involved. It would be interesting to see if morphological transitions, similar to those observed in electrodeposition [3,4], can be found in corrosion processes.

In recent years a strong interest has developed in the growth of rough surfaces and interface equations [20,17,21]. The growth of rough surfaces has been described in terms of Langevin equations [20,17,21] such as the Edwards-Wilkinson [22] and Kardar-Parisi-Zhang [23] (KPZ) equations. These and similar continuum limit surface growth equations have been used to define universality classes for the growth of rough surfaces. Although the KPZ equation would be an attractive starting point for a theoretical analysis of our experimental results the data presented in this paper indicate that the Hurst exponent is larger than the value of $\frac{1}{2}$ expected for $(1+1)$-dimensional surface growth processes in the KPZ universality class. Perhaps micropitting events provide a source of non-Gaussian noise [24,25] and raise the Hurst exponent.

In conclusion, these experimental results show that the morphology associated with the corrosion of aluminum in chloride containing solutions can be described in terms of self-affine fractal geometry.

We gratefully acknowledge support by VISTA, a research cooperation between the Norwegian Academy of Science and Letters and Den norske stats oljeselskap a.s. (STATOIL) and by NAVF, the Norwegian Research Council for Science and the Humanities.

[1] B. B. Mandelbrot, *The Fractal Geometry of Nature* (Freeman, San Francisco, 1982).
[2] J. Feder, *Fractals* (Plenum, New York, 1988).
[3] D. Grier, E. Ben-Jakob, R. Clarke, and L. M. Sander, Phys. Rev. Lett. **56**, 1264 (1986).
[4] V. Fleury, M. Rosso, J.-N. Chazalviel, and B. Sapoval, Phys. Rev. A **44**, 6693 (1991).
[5] K. Sieradzki, R. R. Corderman, K. Shukla, and R. C. Newman, Philos. Mag. A **59**, 713 (1989).
[6] P. Meakin, T. Jøssang, and J. Feder, Physica A **196**, 481 (1993).
[7] T. Nagatani, Phys. Rev. Lett. **68**, 1616 (1992).
[8] P. Meakin, T. Jøssang, and J. Feder, Phys. Rev. E **48**, 2906 (1993).
[9] J. Krug and P. Meakin, Phys. Rev. Lett. **66**, 703 (1991).
[10] T. Jøssang and J. Feder, Phys. Scr. **T44**, 9 (1992).
[11] J. M. Costa, F. Sagués, and M. Vilarrasa, Corros. Sci. **32**, 665 (1991).
[12] *Encyclopedia of Electrochemistry of the Elements,* edited by A. J. Bard (Dekker, New York, 1976).
[13] H. Kaesche, Z. Phys. Chem. Neue Folge **34**, 87 (1962).
[14] G. S. Frankel, Corros. Sci. **30**, 1203 (1990).
[15] A. S. Elola, T. F. Otero, and A. Porro, Corrosion **48**, 854 (1992).
[16] K. P. Wong and R. C. Alkire, J. Electrochem. Soc. **137**, 3010 (1990).
[17] *Dynamics of Fractal Surfaces,* edited by F. Family and T. Vicsek (World Scientific, Singapore, 1991).

[18] W. H. Press, B. P. Flannery, S. A. Teukolsky, and W. T. Vetterling, *Numerical Recipes in C* (Cambridge University Press, Cambridge, England, 1988).
[19] B. B. Mandelbrot, Phys. Scr. **32**, 257 (1985).
[20] J. Krug and H. Spohn, in *Solids far from Equilibrium: Growth Morphology and Defects,* edited by C. Godréche (Cambridge University Press, Cambridge, England, 1991).
[21] P. Meakin, Phys. Rep. **235**, 189 (1993).
[22] S. F. Edwards and D. R. Wilkinson, Proc. R. Soc. London **381**, 17 (1982).
[23] M. Kardar, G. Parisi, and Y.-C. Zhang, Phys. Rev. Lett. **56**, 889 (1986).
[24] Y.-C. Zhang, J. Phys. (Paris) **51**, 2129 (1990).
[25] Y.-C. Zhang, Phys. Rev. B **42**, 4897 (1990).

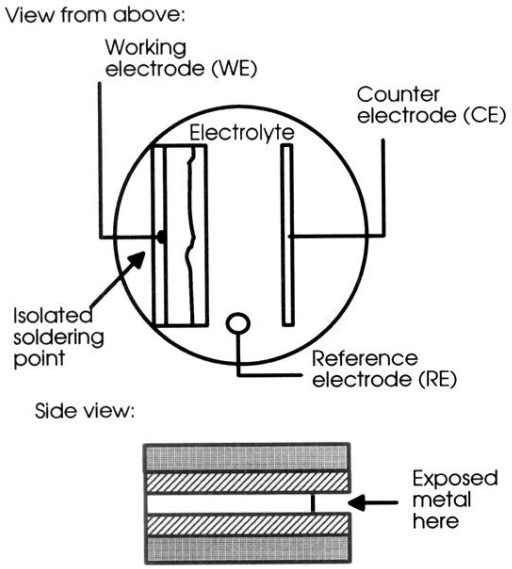

FIG. 1. A schematic representation of the experimental set-up. Above: The cell is viewed from above. Below: The corrosion cell, viewed from one side. Additional glass slides were added on top of and beneath the cell to prevent electrolyte and corrosion products from obscuring the view.

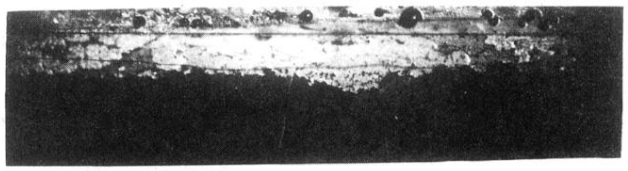

(a)

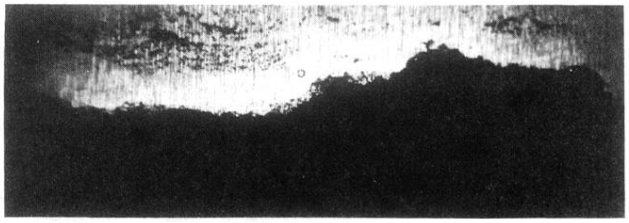

(b)

FIG. 3. Two photographs of aluminum corrosion fronts in a 1*M* NaCl (pH = 12) solution (the metal is black). The potentials were (a) 0.0 V (SCE), and (b) 1.6 V (SCE). These pictures show the parts of the corrosion fronts that were analyzed. Six partly overlapping pictures from each front shown were fitted together to obtain a high resolution image. The horizontal scale is about 14 mm and consists of about 14 000 pixels.